Neurogenetics (2007) 8:1–10
DOI 10.1007/s10048-006-0068-7

ORIGINAL ARTICLE

A null mutation in VAMP1/synaptobrevin is associated with neurological defects and prewean mortality in the lethal-wasting mouse mutant

Arne M. Nystuen · Jamie K. Schwendinger · Andrew J. Sachs · Andy W. Yang · Neena B. Haider

Received: 20 July 2006 / Accepted: 2 October 2006 / Published online: 11 November 2006

Abstract The soluble N-ethylmaleimide sensitive factor attachment receptors are a large family of membrane-associated proteins that are critical for Ca^{2+}-mediated synaptic vesicle release. This family includes the VAMP, synaptosomal-associated protein, and syntaxin proteins. In this report, we describe a mutation in vesicle-associated membrane protein 1(*VAMP1*)/synaptobrevin in the mouse neurological mutant lethal-wasting (*lew*). The lethal-wasting mutant phenotype is characterized by a general lack of movement and wasting, eventually leading to death before weaning. Mutants are visibly immobile and lay on their side by postnatal day 10 (P10). Before this stage, mutants can be identified by a failure to attempt to right themselves. Affected mice die on average at P15. We used a positional cloning strategy to identify the mutation associated with this neurological phenotype. Lethal wasting had previously been linked to chromosome 6. We further narrowed the genetic disease interval and selected a small number of candidate genes for mutation screening. Genes were evaluated by quantitative reverse transcription–polymerase chain reaction (RT–PCR) to detect differences in their expression levels between control and mutant brain ribonucleic acid (RNA) samples. *VAMP1* mRNA was found to be significantly downregulated in the lethal-wasting brain compared to wild-type littermates. Subsequently, a nonsense mutation was identified in the coding region of the gene. This mutation is predicted to truncate approximately half of the protein; however, Western blot analysis showed that no protein is detectable in the mutant. *VAMP1* is selectively expressed in the retina and in discrete areas of the brain including the zona incerta and rostral periolivary region, although no gross histological abnormalities were observed in these tissues. Taken together, these data indicate that *VAMP1* has a vital role in a subset of central nervous system tissues.

Keywords VAMP1 · Lethal-wasting mouse mutant · SNARE complex · Mutation identification · Zona incerta · Rostral periolivary region

A. M. Nystuen (✉) · J. K. Schwendinger · A. J. Sachs · A. W. Yang · N. B. Haider
The Department of Genetics, Cell Biology and Anatomy, 6008 Durham Research Center, University of Nebraska Medical Center, Omaha, NE 68198, USA
e-mail: anystuen@unmc.edu

N. B. Haider
Department of Ophthalmology, 6008 Durham Research Center, University of Nebraska Medical Center, Omaha, NE 68198-5805, USA

Introduction

Changes in intracellular Ca^{2+} levels control a variety of cellular functions, including neurotransmitter release from synaptic vesicles [1–3]. This process involves the fusion of lipid bilayers between a vesicle and the plasma membrane. The soluble N-ethylmaleimide sensitive factor attachment receptor (SNARE) proteins are a large family of membrane-associated proteins that are critical for synaptic vesicle fusion [4–6]. The heterotrimeric SNARE complex is formed by syntaxin 1, synaptosomal-associated protein 25 kDa (SNAP25), and vesicle-associated membrane protein (VAMP)/synaptobrevin [7]. Botulinum and tetanus toxins cleave VAMP1 and VAMP2 to inhibit neurotransmitter release, defining the important role of this complex during vesicle fusion [8–12]. However, the SNAREs are unlikely to represent a minimal fusion complex as multiple proteins are involved in this cellular event. The SNARE proteins are membrane embedded and form transcom-

plexes, bringing the vesicle in close proximity to the plasma membrane [13, 14]. Early evidence demonstrated that changes in intracellular Ca^{2+} levels regulate the process of vesicle fusion; however, the SNARE complex does not bind Ca^{2+} directly. Ca^{2+} was shown to trigger SNARE complex formation in pheochromocytoma 12 cells [15]. The results of several studies have suggested that synaptotagmin [16–18] and calmodulin [19] are the Ca^{2+} sensors that regulate vesicle fusion through the SNARE complex. Calmodulin was shown to directly interact with VAMP2 and regulate exocytosis [20–22]. The calmodulin interaction domain was localized to amino acids 77–94 of VAMP2, downstream of the tetanus toxin cleavage site [23].

In the mouse, there are six VAMPs (also known as synaptobrevin) and an additional seven proteins that have a synaptobrevin domain. Knockout mutants have been produced for *VAMP2*, *VAMP3*, and *VAMP8*. *VAMP2* mutants die immediately after birth and show no detectable histopathology. Neurons in the affected mice show a drastic reduction in Ca^{2+}-triggered vesicle fusion [24]. Consistent with the severity of the mutant phenotype, *VAMP2* is extensively expressed in the central nervous system (CNS; Gene Expression Nervous System Atlas [GENSAT] image no. 47595). *VAMP8* knockout mice develop normally but have pancreatic abnormalities. The affected mice have severe defects in the exocytosis of zymogen granules from acinar cells [25]. The *VAMP3* knockout mouse had no detectable mutant phenotype despite extensive evaluation [26], suggesting the existence of functional redundancy. None of these knockouts exhibit any sort of developmental defect, indicating that the *VAMP* genes are not required for embryonic development. Together, these in vivo models have been useful for functional studies of the VAMPs and have shaped the present understanding of SNARE-mediated vesicle fusion. Mutations in the other *VAMP* genes have yet to be reported; however, the phenotype and underlying molecular mechanisms of pathology should be predictable based on these data and on the knowledge of the expression pattern of the gene family. The expression pattern of *VAMP1* in the rat brain is restricted [27], which suggests that the phenotype of a mouse with a *VAMP1* mutation would also be limited.

In this report, we describe the identification of a nonsense mutation in *VAMP1*/synaptobrevin associated with the lethal-wasting mutant phenotype. The lethal-wasting (*lew*) mutant spontaneously arose at the Jackson laboratory in 1985 on a C3H/HeSnJ background. Lethal wasting is inherited in an autosomal recessive manner and manifests as a neurological phenotype. At 2 weeks postpartum, the mutant displays neurological signs such as curling its front paws inward and clasping its back legs tightly together. The affected mice can move their limbs although not in any purposeful manner. Near P12, the mutants are noticeably immobile, lay on their side, and die preweaning. The gross histopathological examination of the brain showed no lesions. This disorder was linked to a relatively large region on chromosome 6 [28]. A positional cloning strategy was used to identify this mutation; however, rather than extensive breeding to genetically narrow the region, we used informatics resources to select candidate genes from a relatively large genetic region. In this manuscript, we report the identification of a nonsense mutation in *VAMP1* that is associated with the lethal-wasting phenotype. The mutant is a true null, as VAMP1 is not detected in mutant tissues. The expression pattern of *VAMP1* in the mouse suggests a limited but vital group of neurons that are dysfunctional in the lethal-wasting mutant.

Materials and methods

Genotyping and husbandry

All animals were bred and maintained under standard conditions at the University of Nebraska Medical Center (UNMC) research vivarium in accordance with the Institutional Animal Care and Use Committees standards. A mating cross of C3H/HeDiSnJ^{lew}×CAST/EiJ was established to generate F1 mice for an intercross progeny testing. The matings that produced affected offspring were maintained as a mapping cross to generate F2 mice for genotyping. The offspring were counted and visually observed daily until weaning age to determine if perinatal or in utero lethality occurred. Deoxyribonucleic acid (DNA) was isolated from tail tips excised from 10-day-old F2 pups. Approximately one eighth of an inch of tail was excised and then incubated overnight at 55°C in 650 µl of tail digestion buffer (50 mM Tris, 400 mM NaCl, 100 mM ethylenediamine tetraacetic acid, 0.5% sodium dodecyl sulfate (SDS), and 400 µg proteinase K). After the tail tip was fully digested, 175 µl of 6 M NaCl was added and mixed thoroughly. Samples were centrifuged at 14,000×*g* for 20 min. Supernatant was recovered and added to an equal volume of 100% ethanol. The DNA was pelleted by centrifugation at 14,000×*g* for 10 min, dried, and resuspended in ultrapure H_2O to a final concentration of 40 ng/µl.

The offspring were genotyped with several short tandem repeat polymorphism markers in the disease region using a standard PCR protocol. Briefly, DNA was amplified by PCR using the following conditions: 40 ng of template DNA in a 10 µl PCR reaction mixture containing 1.0 µl PCR buffer (100 mM Tris-HCl [pH 8.8], 500 mM KCl, 15 mM $MgCl_2$, and 0.01% w/v gelatin); 200 µM each deoxyadenosine triphosphate, deoxycytidine triphosphate, deoxyguanosine triphosphate, and deoxythimidine triphos-

phate; 2.5 pmol of each forward and reverse primer; and 0.25 U Taq polymerase. Reaction mixtures were subjected to 40 cycles of 94°C for 30 s, 53°C for 60 s, and 72°C for 60 s. Amplification products were electrophoresed at 100 V for 1 h on a 4% agarose gel containing 0.5 μg/ml ethidium bromide and visualized by ultraviolet transillumination. C3H/HeDiSnJ and CAST/EiJ control DNAs were included in each set of reactions for proper sizing of strain-specific alleles to ensure proper genotyping.

Expression analysis

Quantitative RT–PCR was used to determine relative expression levels of candidate genes. Total brain ribonucleic acid (RNA) was isolated from four mutant and control littermates using Trizol reagent (Invitrogen) per manufacturer's instructions. The RNA was DNase treated with DNA-free (Ambion) to remove the contaminating DNA, per manufacturer's instructions. First, strand synthesis was performed using the RETROscript kit (Ambion) on 2 μg of RNA template, per manufacturer's instructions. Reaction products were diluted 1 to 100, and 1 μl was used as template for amplification using the following 10-μl-reaction mixture: 100 pmol each forward and reverse primer, and 6 μl Sybr Green PCR master mix (ABI). Forward and reverse primers were chosen for each gene using Primer Express 3.0 (ABI). Quantitative PCR was carried out on an ABI 7500 using the default cycling parameters. Reactions were performed in triplicate for the four separate RNA samples for wild type and mutant. As a measure of amplification, the number of cycles to a manually set ΔR_n (dye fluorescence) threshold was determined as the ΔC_t value (ABI 7500 system software). ΔC_t values were obtained for each sample, a total of 12 for each gene (four triplicated replicates). The average ΔC_t for each gene was calculated for each data set, as well as the standard deviation and standard error. Significance was determined by the *t*-test. The $\Delta\Delta C_t$ was derived by comparison to a control gene, β-actin, for each sample. Comparisons between mutant and wild-type control samples were made for fold-change estimation using the comparative C_t method, $2^{-\Delta\Delta C_t}$, where $\Delta\Delta C_t = \Delta C_t$ test gene-ΔC_tβ-actin; relative expression was calculated per 1,000 molecules of β-actin, $1,000/2^{-\Delta\Delta C_t}$.

Mutation analysis

Mutation analysis was performed by directly sequencing RT–PCR products amplified from RNA and confirmed by sequencing PCR products amplified from genomic DNA. RT–PCR primers were designed from exon sequences of *VAMP1* to amplify several fragments across the coding region. RT–PCR was carried out on mutant and wild-type RNA from multiple tissues using the Titan one-tube RT–PCR system (Roche). Amplified products were recovered and sequenced as stated below. For confirmation of the mutation, we sequenced genomic DNA using primers that were designed flanking the exons of *VAMP1*. DNA was amplified as before. For the strain survey, DNA samples from several strains were purchased from the Jackson Laboratory mouse DNA resource. The appropriate bands were excised, and DNA was recovered using the Qiagen gel extraction kit, per manufacturer's instructions. The recovered fragments were sequenced by the DNA-sequencing core at UNMC. Sequence analysis was performed using Sequencher 4.5 (gene codes). Protein sequence analysis was performed using Clustal [29].

Histology

Tissues were fixed via transcardial perfusion of the mouse. Tissues were removed from mutant and age-matched 14-day-old littermates and fixed in 3.7% paraformaldehyde. Tissues were paraffin embedded by the Eppley Center Histology Core. Tissues were sectioned in the sagittal plane at 8 μm thick on a Lieca RM2135 microtome. Sections were mounted on poly-L-lysine-coated slides. Hematoxylin and eosin staining was performed as before for general histological analysis of the tissue [30]. Sections were visualized under bright-field on a Ziess AxioPlan 2 and imaged with the Ziess AxioCam using Axiovision 4.3 software.

Western blot analysis

The Western blot analysis was performed using 20 μg of protein per sample. A control and a mutant brain were dissected from postnatal day 14 (P14) mice and homogenized in radioimmunoprecipitation buffer (1×Tris buffered saline, 1% NP-40, 0.5% sodium deoxycholate, 0.1% SDS, 0.04% sodium azide, 1 mM phenylmethylsulphonylflouride, 1×complete protease inhibitor cocktail [Roche]) using an Ika ultra-turrax T8 homogenizer at 4,000 rpm. Samples were centrifuged at 14,000×*g* for 20 min at 4°C to remove debris. The supernant was boiled for 10 min in NuPAGE lithium dodecyl sulfate sample buffer (Invitrogen) and electrophoresed at 200 V for 30 min on 12% Tris-Bis NuPAGE gels (Invitrogen). Gels were equilibrated in 1× NuPAGE transfer buffer (Invitrogen). Proteins were transferred onto equilibrated polyvinylidenfluoride membranes using the X-Cell II Blot Module (Invitrogen), per manufacturer's instructions. Transfer was performed at 30 V for 2 h at room temperature in transfer buffer. After transfer, blots were washed in phosphate-buffered saline (PBS) and then incubated in Odyssey blocking solution (LiCor Technologies) for 1 h at room temperature. Primary

antibody was diluted in Odyssey blocking solution, anti-VAMP1 at 1:3,000 (Abcam) or anti-β-actin at 1:1,000 (Santa Cruz), and incubated on the membrane overnight at 4°C. The blot was then washed in three changes of PBS. The appropriate secondary antibody was incubated on the membrane at 1:5,000 in Odyssey blocking solution for 1 h at room temperature (AlexaFluor680 [Molecular Probes] or IRDye800CW [Rockland]). Images were detected with the Odyssey infrared imaging system (LiCor Technologies) using the proper infrared channels and visualized using Odyssey v.1.2 software.

Immunohistochemistry

Immunohistochemistry was performed as before [31] using an antibody specific to VAMP1 (Abcam). Control and mutant P14 mice were fixed via transcardial perfusion, and brains were dissected. Tissues were prepared and sectioned as before. Slides were treated in the following washes to deparaffinize and hydrate the sections: xylene, 10 min, two changes; 100% ethanol, 5 min, two changes; 95% ethanol, 5 min; 70% ethanol, 3 min; PBS, 5 min. Tissue sections were blocked in 1×PBS, 0.1% Tween, 5% goat serum for 1 h, then incubated with primary antibody (1:1,000) in blocking solution overnight at 4°C in a humidified chamber. The slides were washed with three changes of PBS for 5 min each and then incubated with secondary antibody, AlexaFlor 488 (Molecular Probes), 1:200 in blocking solution. Slides were washed in three changes of PBS for 5 min each and briefly counterstained with 4′,6-diamidino-2-phenylindole (Sigma) 1:200 in PBS, washed in PBS again, and mounted with Vectashield (Vector Laboratories). Sections were visualized by florescent microscopy on a Ziess AxioPlan 2 and imaged with the Ziess AxioCam using Axiovision 4.3 software.

Results

Characterization of the lethal-wasting phenotype

Lethal-wasting is an autosomal recessive mutation. In the mapping cross, we observed 25.6% affected mice with no indication of in utero loss or immediate death after birth. The affected mice die near P15. By P10, the mutants are noticeably immobile and lay on their side. The mutants fail to attempt to right when placed on their backs; otherwise, in earlier perinatal stages, the mutants are of normal size and difficult to discern from their normal littermates. The affected mice can move their limbs although not in any purposeful manner. Hematoxylin and eosin were used to stain brain sections. No gross histological defects were observed (data not shown).

Genetic mapping of the lethal-wasting mutation

The lethal-wasting disease interval was reported to be between markers D6Mit55 and D6Mit111, a distance of approximately 20 mb, containing more than 200 genes. We created a C3H/HeDiSnJ^{lew}×CAST/EiJ cross to generate a total of 256 F2 offspring for genetic fine mapping. The disease region was narrowed to approximately 1 mb by mapping recombination events that had occurred in five F2 offspring (Fig. 1). Recombination events had occurred in three unaffected mice that were progeny tested to ascertain carrier status. Mouse 127 never had affected offspring when mated to an obligate heterozygote (0 out of 27 pups), whereas mouse 242 did have affected offspring. Their recombination events both mapped between markers D6Mit193 and D6Mit24, thus excluding everything proximal to D6Mit193. Mouse 252 was unaffected and homozygous for the C3H/HeDiSnJ chromosome at markers D6Jpk2 and D6Mit334, thus excluding everything distal to these markers. Three markers remained completely linked with the disease phenotype. The Ensembl genome browser was used to identify the genes between markers D6Mit193 and D6Jpk2. Several informatics tools were used to evaluate all 41 of the genes within the interval. Nineteen of the genes had been previously associated with a disparate mutant phenotype in the mouse. Of the remaining genes, five were chosen for mutation screening based on a predominantly neuronal expression pattern and putative function (Table 1).

Identification of a nonsense mutation in *VAMP1*

It is generally thought that approximately 30% of known mutations in the mouse results in a disruption of the expression of the gene. Thus, an efficient first-pass mutation screen was performed on five genes using quantitative RT–PCR (qRT–PCR) to detect differences in their relative expression between mutant and wild-type tissues. Total RNA was isolated from four mutant and four wild-type brains and used as template for qRT–PCR. Five genes were evaluated: atrophin 1, *VAMP1*, enolase 2, guanine nucleotide-binding protein, beta 3, and G protein-coupled receptor 162. β-Actin was used as a control and a benchmark for the determination of fold change between mutant and wild-type message levels. *VAMP1* mRNA levels were significantly decreased ($p<0.001$) in mutant brains compared to wild-type littermates (Table 1). None of the other genes showed any significant differences in their expression levels between mutant and wild-type RNA samples.

VAMP1 was amplified by the RT–PCR from the mutant and control brain RNA and sequenced. A G190T transversion resulting in a premature stop codon was identified in the mutant (Fig. 2a). This mutation was confirmed by

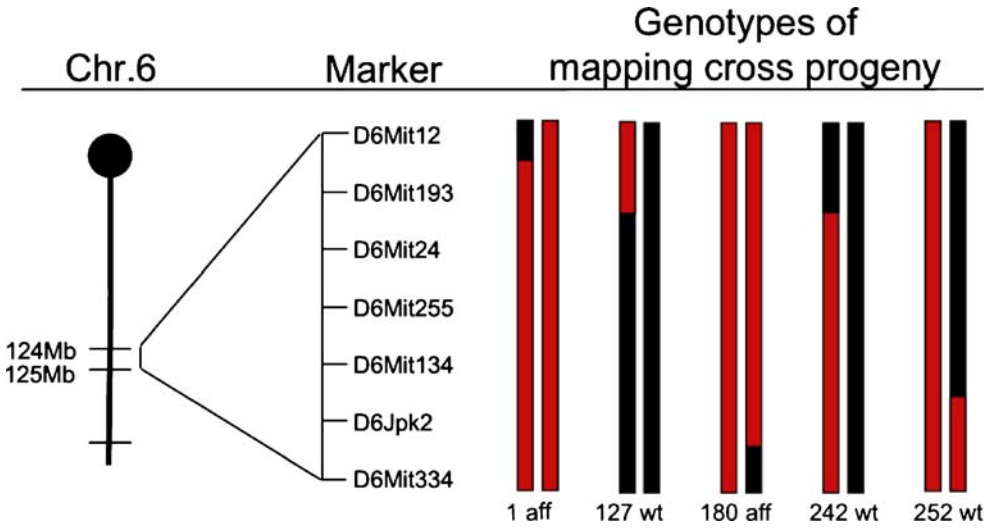

Fig. 1 Genetic map of the lethal-wasting region on chromosome 6. *On the left*, the physical map of chromosome 6 is shown with the genetic markers that were used for fine mapping. *On the right*, five mice that define the critical genetic interval for the disease are shown. Mapped recombination events are depicted as colored chromosomes, the wild type CAST/EiJ chromosome (*black*) and mutation carrying C3H^{lew} chromosome (*red*). The mouse identification number and its phenotype are given (affected [*aff*] and unaffected [*wt*])

sequencing DNA, amplified by the PCR from the heterozygous and affected mice. This mutation was not detected in a strain survey of 20 common laboratory mouse strains, including the strain of origin (data not shown).

Lethal-wasting mice lack VAMP1 protein

The G190T nonsense mutation is predicted to truncate nearly half of the protein. Clustal analysis shows that the VAMP1 protein is highly conserved between species and within the protein family. VAMP1 has several important domains including a transmembrane domain and a calmodulin interaction domain that would be eliminated in the lethal-wasting mutant (Fig. 2b). However, the sharp decrease in mutant mRNA levels suggests that nonsense-mediated degradation of the *VAMP1* message may occur. Western blot analysis was used to detect the presence or absence of a truncated protein. Protein samples from wild-type and mutant brain tissues were probed with an anti-VAMP1 antibody. This antibody was raised to the *N*-terminal 18 amino acids of the rat VAMP1, thereby allowing specificity within the family and detection of the putative lethal-wasting truncated protein. Figure 3a shows that no VAMP1 protein is detectable in the mutant brain. β-Actin was used as a loading control. The lack of VAMP1 in the lethal-wasting mutant was confirmed by immunohistochemistry.

VAMP1 is expressed in the retina and in discrete neuroanatomical regions

In agreement with the lethal-wasting phenotype, RT–PCR using RNA from multiple tissues shows that *VAMP1* is predominantly expressed in neuronal tissues (Fig. 3b). The primers used for the RT–PCR were designed from an area of the 3′ untranslated region that is common to known alternative splice forms. The lethal-wasting mutant phenotype does not indicate which areas of the brain may be affected; therefore, we used immunohistochemistry to identify where VAMP1 is expressed. Mutant and control (P14) tissue samples were sectioned and immunostained with anti-VAMP1 antibody. In wild-type tissue, high VAMP1 expression was detected in the zona incerta and rostral periolivary region (Fig. 4), whereas other neuroanatomical regions showed negligible expression of VAMP1.

Table 1 Candidate gene analysis for genes in the lethal-wasting interval. Five genes were selected based on the expression data from UniGene's EST profile viewer and putative function. Quantitative RT–PCR was used to identify significantly decreased levels of *Vamp1* expression in lethal-wasting mutant tissue compared to wild-type littermates

Gene	Function	Expression	Fold change in mutant
Atrophin 1 (*Atn1*)	Associated with dentatorubral–pallidoluysian atrophy	Widely expressed	Increased 1.19×±0.15 (p=0.095)
Enolase 2 (*Eno2*)	Glycolysis	High in CNS	Increased 1.46×±0.26 (p=0.089)
Guanine nucleotide-binding protein, β3 (*Gnb3*)	Signal transduction	Restricted expression, detectable levels in pineal, eye, and heart	Increased 1.68±0.42 (p=0.070)
G protein-coupled receptor 162 (*Gpr162*)	Signal transduction	High in CNS	Increased 1.19×±0.26 (p=0.148)
Vesicle-associated membrane protein 1 (*Vamp1*)	Synaptic vesicle release	High in CNS	Decreased 4.38×±0.33 (p=0.001)

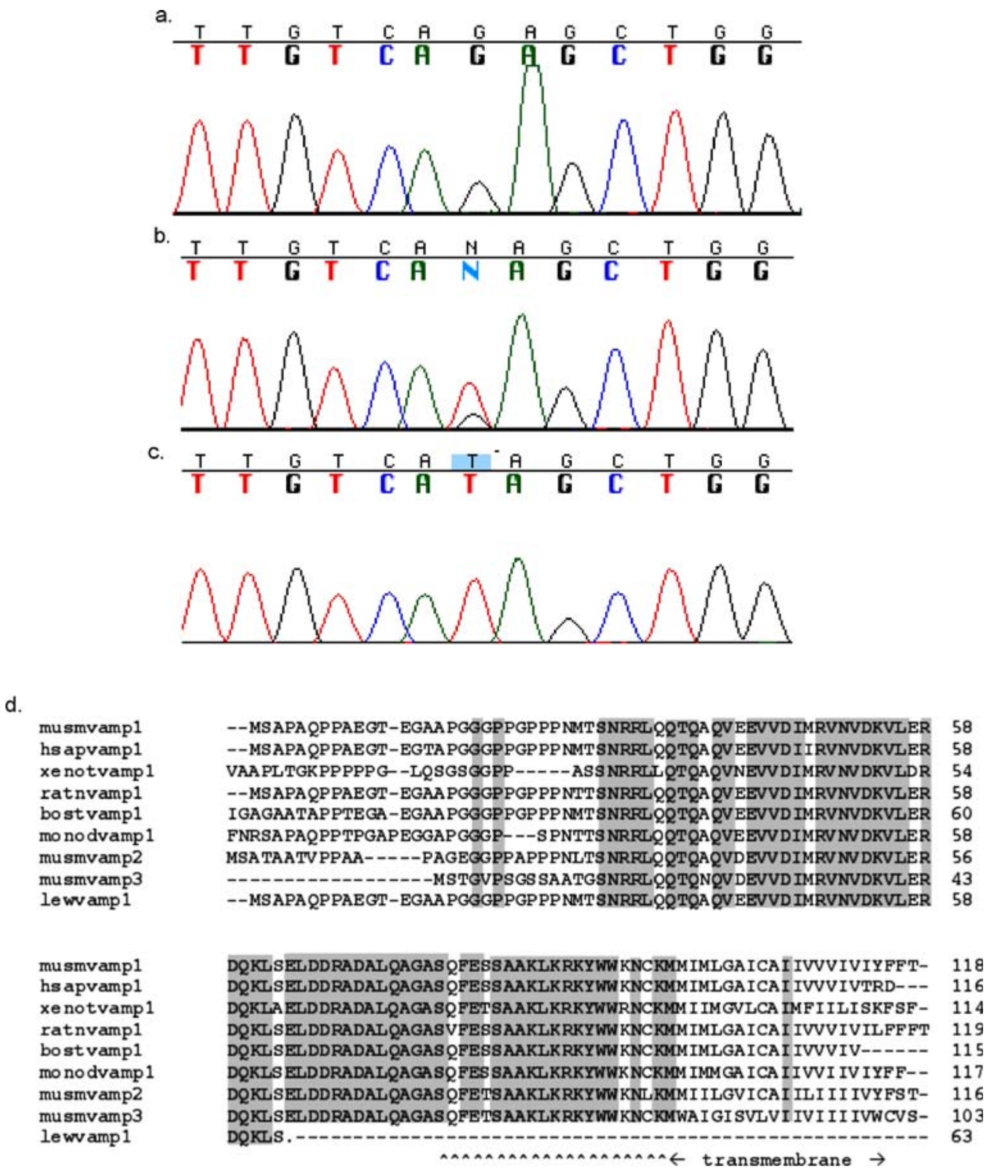

Fig. 2 Identification of a nonsense mutation in *Vamp1* in the lethal-wasting mutant. Sequence chromatograms from wild-type (panel **a**), heterozygous (panel **b**), and mutant (panel **c**) show the G190T transversion (*highlighted in blue*). This mutation truncates VAMP1 upstream of functional domains (panel **d**). VAMP1 amino acid sequences are shown from several species: mouse, human, frog, rat, cow, and opossum. VAMP2 and VAMP3 sequences from the mouse are also shown. *Shaded areas* show blocks of high conservation. The position of the nonsense mutation is noted (*lewvamp1*), as well as the calmodulin interaction domain (^) and the transmembrane domain

In the retina, staining was observed in the outer segments of the photoreceptors, in the outer and inner plexiform layers, and in a subset of ganglion cells. Staining was punctate, excluded from the nucleus and associated with the plasma membrane. As with the Western blot, no immunoreactivity was observed in mutant tissues.

Evaluation of the differential expression of SNARE genes in the lethal-wasting mutant

Lethal-wasting mutant brains were evaluated for the misregulation of the gene expression of other neuronally expressed members of the SNARE complex (syntaxin 1a, *SNAP25*, and syntaxin binding protein 2) and potentially compensating *VAMPs* (synaptobrevin-like 1, also known as *Ti-VAMP* or *VAMP7* and *VAMP2*). Quantitative RT–PCR was performed on RNA isolated from microdissected brain tissues from four mutant and four wild-type littermates. The relative expression levels (transcripts per 1,000 transcripts of β-actin) of the genes were calculated. Although all genes had slightly elevated expression levels in the mutant compared to wild-type, the differences were not statistically significant (Fig. 5).

Discussion

In this study, we report the identification of a mutation in *VAMP1* that is associated with prewean lethality and neurological defects in the lethal-wasting mouse mutant. A nonsense mutation in the *VAMP1* gene was identified. Several lines of evidence support the assertion that this mutation is causal. First, the drastic nature of the mutation eliminates nearly half of the protein, including regions

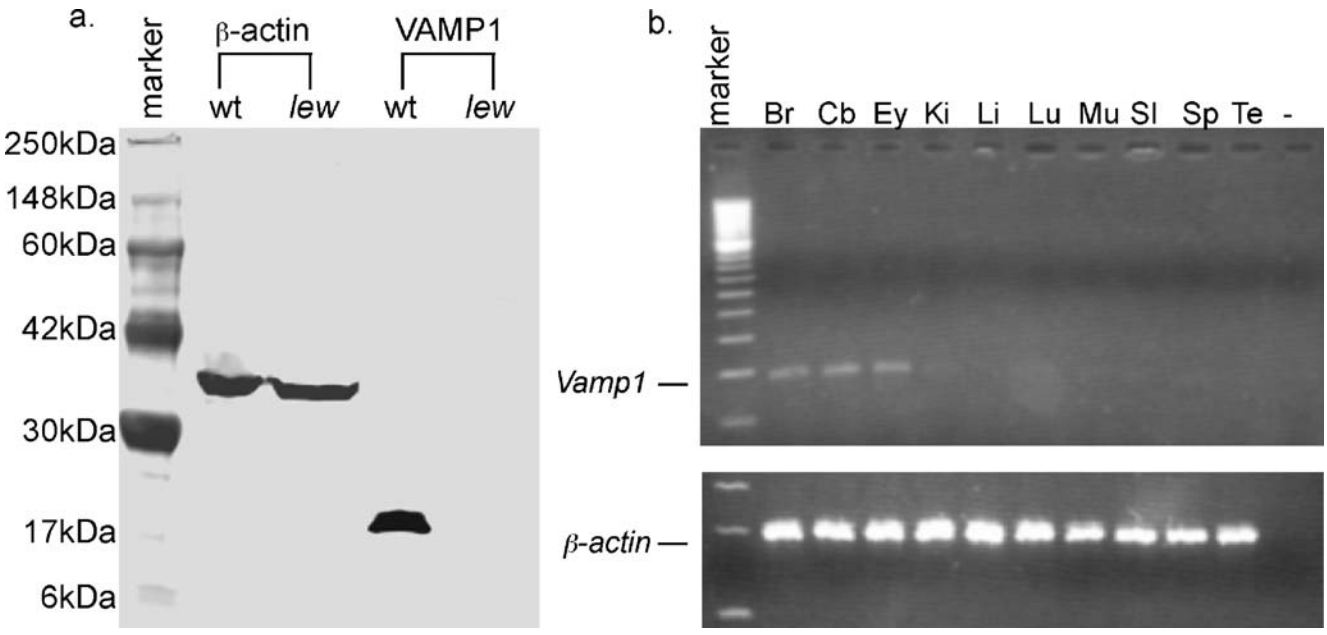

Fig. 3 Western blot analysis shows no detectable protein in the mutant mouse. Protein was isolated from the brain tissue of the mutant and control littermates and used for Western blot analysis (panel **a**). *Lane 4* shows the wild-type protein at the expected size of 17 kDa (*ladder*, *lane 1*). *Lane 5* shows a lack of protein in the mutant. β-Actin is shown as a loading control (*lanes 2* and *3*). Panel **b**, in agreement with the lethal-wasting phenotype, *Vamp1* mRNA is expressed most highly in neuronal tissues; β-actin is shown as a control. RT–PCR was performed on DNase I treated RNA from the indicated tissues: *Br* brain, *Cb* cerebellum, *Ey* eye, *Ki* kidney, *Li* liver, *Lu* lung, *Mu* muscle, *SI* small intestine, *Sp* spleen, *Te* testis, and *minus sign* negative control

putatively cleaved by tetanus and botulinum toxins (peptide cleavage studies were originally performed on rat proteins, which showed that VAMP1 was sensitive to botulinum toxins D, F, and G but not tetanus toxin due to a Q76V amino acid substitution; the mouse does not have this substitution). Additionally, there is a sharp reduction in *VAMP1* mRNA in mutant mouse tissues compared to wild type. Further, the mutant lacks detectable protein in the brain and retina. This was observed using an *N*-terminal antibody that should have detected a truncated protein if it existed. The mutation that we identified inserts a stop codon in the middle of the message and would disrupt all known alternative splice forms of the gene. Importantly, the mutation was not found in the strain of origin or in a strain survey. Finally, nearly half of the genes in the disease interval had already been associated with a phenotype in the mouse. None of these were similar enough to the lethal-wasting phenotype to warrant an allelism test.

The use of qRT–PCR as a first-pass screen of candidate genes allows for the simultaneous screening of several genes. One caveat is that mutant tissue may have several genes misregulated as a result of—and not the cause of—the phenotype. In fact, in the rat, *VAMP1* is downregulated in the facial motor nucleus after axotomy of the facial nerve [32]. In schizophrenic patients, levels of *VAMP1* in the superior temporal gyrus were found to be significantly lower than those of unaffected controls [33]. The results of these studies indicate that abnormalities in the expression of VAMPs may be involved in several dissimilar neurological disorders. A similar phenomenon is seen with the phosphatidylinositol metabolism pathway, which is also essential for the maintenance of normal synaptic vesicle dynamics. Null mutations in genes of this pathway result in dramatic phenotypes [34, 35], but minor disruptions of the pathway, including relatively small expression differences, are thought to be associated with several neurogenetic disorders including autism [36, 37], psychiatric disorders [38, 39], and cognitive defects [40].

The lethal-wasting phenotype is relatively mild compared to that of the *VAMP2* knockout mutant. The expression pattern of *VAMP1* in the brain is far more restricted than *VAMP2*. *VAMP2* is expressed throughout the mouse brain and at extremely high levels in the hippocampus and cortex, whereas relatively lower expression levels are observed in the mes- and diencephalon (GENSAT no. 47593–95). The *VAMP2* knockout mouse dies at birth, whereas the lethal-wasting mutant survives 2 weeks. The reason for this phenotypic difference is not clear, but it is reflective of the fact that *VAMP2* is the predominant VAMP isoform in the brain, and that *VAMP1* expression is restricted to a few regions of the diencephalon and midbrain. The lethal-wasting phenotype also indicates that these neuroanatomical regions are not immediately required for life and are likely still developing during the second postnatal week.

The VAMPs are important for membrane fusion events. Although the lipid bilayer fusion events are not well

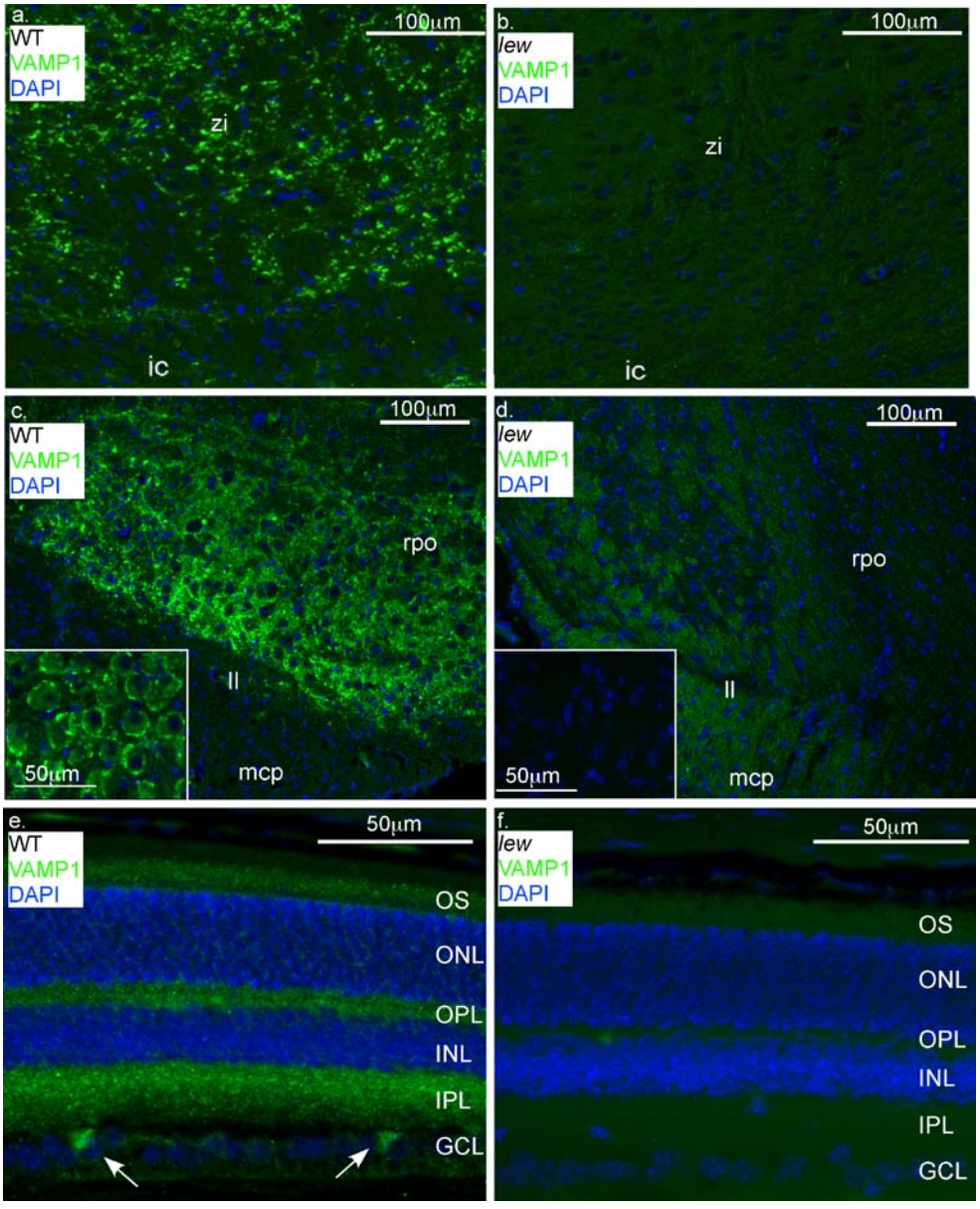

Fig. 4 Immunohistochemistry shows that VAMP1 (*green*) is expressed in the zona incerta, rostral periolivary region, and retina of wild-type mice and lacking in the mutant; however, no gross histological defects are observed in the mutant mouse. The zona incerta (panel **a**), rostral periolivary region (panel **c**), and retina (panel **e**) of a wild-type mouse show strong immunoreactivity with the anti-VAMP1 antibody (*arrows* indicate ganglion cells). Panels **b**, **d**, and **f** demonstrate the lack of immunoreactivity in the matched sections from mutant tissues. The *inset* shows the association of VAMP1 with the plasma membrane. The slides were DAPI counterstained (*blue*). The following abbreviations are used: *zi* zona incerta, *ic* internal capsule, *rpo* rostral periolivary region, *Il* infralimbic cortex, *mcp* middle cerebellar peduncle, *OS* outer segments, *ONL* outer nuclear layer, *OPL* outer plexiform layer, *INL* inner nuclear layer, *IPL* inner plexiform layer, and *GCL* ganglion cell layer

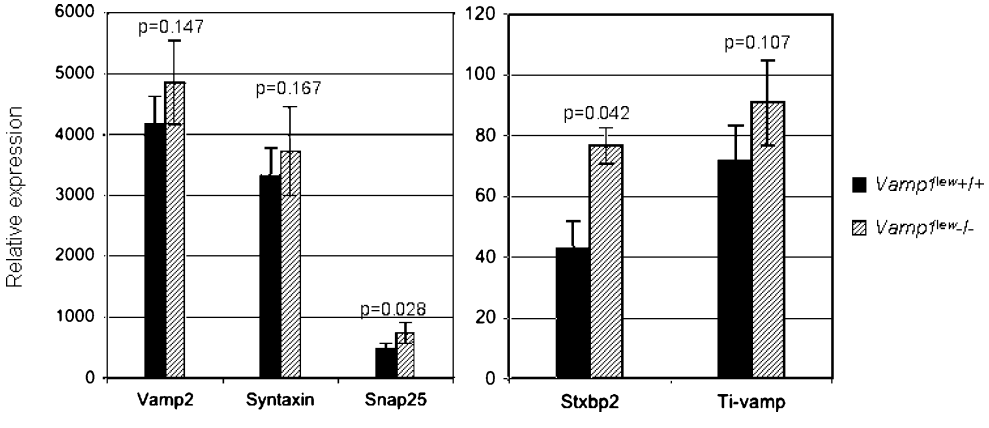

Fig. 5 Expression levels of other SNARE proteins are unchanged in the lethal-wasting mutant. Relative expression levels (number of messages per 1,000 messages of β-actin) are shown for each gene. Statistical significance (*p* value) of the difference in expression is shown *below* the gene

understood, the protein/protein interactions that are necessary for fusion have been thoroughly studied. The VAMPs are members of the SNARE family of proteins that are directly involved in initiating membrane fusion; however, they do not appear to represent a minimal fusion apparatus. Associated proteins from the SM family (Sec1/Munc18-like) are necessary for fusion. A knockout mutation of *Munc-18a* leads to a complete loss of neurotransmitter release [41], whereas deletion of *VAMP2* causes a dramatic reduction, but not complete loss, of vesicle fusion. SM proteins appear to act as regulators of the SNARE assembly, whereas other proteins are involved in the regulation of synaptic vesicle exocytosis. A knockout of the Ca^{2+}-binding protein synaptotagmin in mice shows loss of synchronous release [42]. Ca^{2+} induces the binding of synaptotagmin to SNARE complexes, syntaxin-SNAP25 heterodimers, and both proteins individually [43, 44], as well as phospholipids [45], thus suggesting that synaptotagmin is the major coordinator of synchronous release [46]. VAMP1/2, as members of the SNARE complex, are involved in Ca^{2+}-stimulated synaptic vesicle release; therefore, it is likely that the lethal-wasting mutant has a defect of neurotransmission in a subset of neurons.

In the human, alternative splice forms of VAMP1 have been described with different C-terminals that are involved in the differential targeting of vesicles to subcellular structures [47]. VAMP1A is expressed in the brain and targeted to the plasma membrane, whereas VAMP1B is targeted to the mitochondria and expressed in several cell lines [48]. In the mouse, an expressed sequence tag (EST) evidence exists for the presence of two splice forms equivalent to human VAMP1A and VAMP1B. The lethal-wasting mutation would affect both of these splice forms; therefore, the significance of either splice forms to the lethal-wasting phenotype would be difficult to discern without making a knockout specifically targeting the *VAMP1b* isoform.

VAMP1 is expressed in the retina, zona incerta, and rostral periolivary neurons. In the retina, staining was observed in the inner and outer plexiform layers, and in a subset of ganglion cells, consistent with a previous report [49]. However, we also observed staining in the outer segments. The function of *VAMP1* in the retina is unclear, as the expression pattern of *VAMP1* in the retina appears to be somewhat duplicated by *VAMP2*. It is yet unknown whether lethal-wasting mutants have visual defects; however, unlike the *VAMP2* knockout mutant, electroretinogram analysis will be possible on lethal-wasting mutants. The function of the zona incerta is not completely understood. It receives input from the precentral gyrus of the cerebral cortex and cerebellum, suggesting a role in movement, which would be consistent with the lethal-wasting phenotype. The rostral periolivary region receives input from the inferior colliculus, a major auditory processing center [50]. Thus, the lethal-wasting mouse will not only be a valuable resource for the study of vesicle fusion but for the study of discrete neuroanatomical regions for which functional information is limited.

Acknowledgment The DNA sequencing core at UNMC receives partial support from the National Institutes of Health grant number P20 RR016469 from the Idea Network of Biomedical Research Excellence program of the National Center for Research Resources.

References

1. Burgoyne RD, Morgan A (1995) Ca2+ and secretory-vesicle dynamics. Trends Neurosci 18:191–196
2. Pelham HR (2001) SNAREs and the specificity of membrane fusion. Trends Cell Biol 11:99–101
3. Coorssen JR, Blank PS, Albertorio F, Bezrukov L, Kolosova I, Chen X, Backlund PS Jr, Zimmerberg J (2003) Regulated secretion: SNARE density, vesicle fusion and calcium dependence. J Cell Sci 116:2087–2097
4. Chen YA, Scheller RH (2001) SNARE-mediated membrane fusion. Nat Rev Mol Cell Biol 2:98–106
5. Gerst JE (1999) SNAREs and SNARE regulators in membrane fusion and exocytosis. Cell Mol Life Sci 55:707–734
6. Jahn R, Sudhof TC (1999) Membrane fusion and exocytosis. Annu Rev Biochem 68:863–911
7. Sollner T, Bennett MK, Whiteheart SW, Scheller RH, Rothman JE (1993) A protein assembly–disassembly pathway in vitro that may correspond to sequential steps of synaptic vesicle docking, activation, and fusion. Cell 75:409–418
8. Niemann H, Blasi J, Jahn R (1994) Clostridial neurotoxins: new tools for dissecting exocytosis. Trends Cell Biol 4:179–185
9. Schiavo G, Matteoli M, Montecucco C (2000) Neurotoxins affecting neuroexocytosis. Physiol Rev 80:717–766
10. Schiavo G, Malizio C, Trimble W, Polverino P, Milan G, Sugiyama C, Johnson EA, Montecucco C (1994) Botulinum-G neurotoxin cleaves VAMP/synaptobrevin at a single Ala–Ala peptide bond. J Biol Chem 269:20213–20216
11. Verderio C, Coco S, Bacci A, Rossetto O, De Camilli P, Montecucco C, Matteoli M (1999) Tetanus toxin blocks the exocytosis of synaptic vesicles clustered at synapses but not of synaptic vesicles in isolated axons. J Neurosci 19:6723–6732
12. Schiavo G, Benfenati F, Poulain B, Rossetto O, Polverino P, DasGupta B, Montecucco C (1992) Tetanus and botulinum-B neurotoxins block neurotransmitter release by proteolytic cleavage of synaptobrevin. Nature 359:832–835
13. Rizo R, Chen X, Arac D (2006) Unraveling the mechanisms of synaptotagmin and SNARE function in neuro transmitter release. Trends Cell Biol 16:339–350
14. Jahn R, Lang T, Sudhof TC (2003) Membrane fusion. Cell 112:519–533
15. Chen YA, Scales SJ, Patel SM, Doung YC, Scheller RH (1999) SNARE complex formation is triggered by Ca2+ and drives membrane fusion. Cell 97:165–174
16. Fernandez-Chacon R, Konigstorfer A, Gerber SH, Garcia J, Matos MF, Stevens CF, Brose N, Rizo J, Rosenmund C, Sudhof TC (2001) Synaptotagmin I functions as a calcium regulator of release probability. Nature 410:41–49
17. Mackler JM, Drummond JA, Loewen CA, Robinson IM, Reist NE (2002) The C(2)B Ca(2+)-binding motif of synaptotagmin is required for synaptic transmission in vivo. Nature 418:340–344

18. Tucker WC, Weber T, Chapman ER (2004) Reconstitution of Ca2+-regulated membrane fusion by synaptotagmin and SNAREs. Science 304:435–438
19. Peters C, Mayer A (1998) Ca2+/calmodulin signals the completion of docking and triggers a late step of vacuole fusion. Nature 396:575–580
20. Quetglas S, Leveque C, Miquelis R, Sato K, Seagar M (2000) Ca2+-dependent regulation of synaptic SNARE complex assembly via a calmodulin- and phospholipid-binding domain of synaptobrevin. Proc Natl Acad Sci U S A 97:9695–9700
21. De Haro L, Quetglas S, Iborra C, Leveque C, Seagar M (2003) Calmodulin-dependent regulation of a lipid binding domain in the v-SNARE synaptobrevin and its role in vesicular fusion. Biol Cell 95:459–464
22. de Haro L, Ferracci G, Opi S, Iborra C, Quetglas S, Miquelis R, Leveque C, Seagar M (2004) Ca2+/calmodulin transfers the membrane-proximal lipid-binding domain of the v-SNARE synaptobrevin from cis to trans bilayers. Proc Natl Acad Sci U S A 101:1578–1583
23. Quetglas S, Iborra C, Sasakawa N, De Haro L, Kumakura K, Sato K, Leveque C, Seagar M (2002) Calmodulin and lipid binding to synaptobrevin regulates calcium-dependent exocytosis. EMBO J 21:3970–3979
24. Schoch S, Deak F, Konigstorfer A, Mozhayeva M, Sara Y, Sudhof TC, Kavalali ET (2001) SNARE function analyzed in synaptobrevin/VAMP knockout mice. Science 294:1117–1122
25. Wang CC, Ng CP, Lu L, Atlashkin V, Zhang W, Seet LF, Hong W (2004) A role of VAMP8/endobrevin in regulated exocytosis of pancreatic acinar cells. Dev Cell 7:359–371
26. Yang C, Mora S, Ryder JW, Coker KJ, Hansen P, Allen LA, Pessin JE (2001) VAMP3 null mice display normal constitutive, insulin- and exercise-regulated vesicle trafficking. Mol Cell Biol 21:1573–1580
27. Raptis A, Torrejon-Escribano B, Gomez de Aranda I, Blasi J (2005) Distribution of synaptobrevin/VAMP 1 and 2 in rat brain. J Chem Neuroanat 30:201–211
28. Harris B, Ward PF, Johnson KR, Bronson RT, Davisson MT (2003) Lethal wasting (*lew*), a new mouse mutation causing prewean lethality. http://www.jax.org/mmr
29. Chenna R, Sugawara H, Koike T, Lopez R, Gibson TJ, Higgins DG, Thompson JD (2003) Multiple sequence alignment with the Clustal series of programs. Nucleic Acids Res 31:3497–3500
30. Nystuen A, Legare ME, Shultz LD, Frankel WN (2001) A null mutation in inositol polyphosphate 4-phosphatase type I causes selective neuronal loss in weeble mutant mice. Neuron 32:203–212
31. Haider NB, Naggert JK, Nishina PM (2001) Excess cone cell proliferation due to lack of a functional NR2E3 causes retinal dysplasia and degeneration in rd7/rd7 mice. Hum Mol Genet 10:1619–1626
32. Che YH, Yamashita T, Tohyama M (2002) Changes in mRNA for VAMPs following facial nerve transection. J Chem Neuroanat 24:147–152
33. Sokolov BP, Tcherepanov AA, Haroutunian V, Davis KL (2000) Levels of mRNAs encoding synaptic vesicle and synaptic plasma membrane proteins in the temporal cortex of elderly schizophrenic patients. Biol Psychiatry 48:184–196
34. Cremona O, Di Paolo G, Wenk MR, Luthi A, Kim WT, Takei K, Daniell L, Nemoto Y, Shears SB, Flavell RA, McCormick DA, De Camilli P (1999) Essential role of phosphoinositide metabolism in synaptic vesicle recycling. Cell 99:179–188
35. Di Paolo G, Moskowitz HS, Gipson K, Wenk MR, Voronov S, Obayashi M, Flavell R, Fitzsimonds RM, Ryan TA, De Camilli P (2004) Impaired PtdIns(4,5)P2 synthesis in nerve terminals produces defects in synaptic vesicle trafficking. Nature 431:415–422
36. Friedman SD, Shaw DW, Artru AA, Richards TL, Gardner J, Dawson G, Posse S, Dager SR (2003) Regional brain chemical alterations in young children with autism spectrum disorder. Neurology 60:100–107
37. Serajee FJ, Nabi R, Zhong H, Mahbubul Huq AH (2003) Association of INPP1, PIK3CG, and TSC2 gene variants with autistic disorder: implications for phosphatidylinositol signalling in autism. J Med Genet 40:e119
38. Levine J (1997) Controlled trials of inositol in psychiatry. Eur Neuropsychopharmacol 7:147–155
39. Einat H, Belmaker RH (2001) The effects of inositol treatment in animal models of psychiatric disorders. J Affect Disord 62: 113–121
40. Di Paolo G, Sankaranarayanan S, Wenk MR, Daniell L, Perucco E, Caldarone BJ, Flavell R, Picciotto MR, Ryan TA, Cremona O, De Camilli P (2002) Decreased synaptic vesicle recycling efficiency and cognitive deficits in amphiphysin 1 knockout mice. Neuron 33:789–804
41. Verhage M, Maia AS, Plomp JJ, Brussaard AB, Heeroma JH, Vermeer H, Toonen RF, van den Berg TK, Misler M, Geuze HJ, Sudhof TC (2000) Synaptic assembly of the brain in the absence of neurotransmitter secretion. Science 287:864–869
42. Geppert M, Goda Y, Hammer RE, Li C, Rosahl TW, Stevens CF, Sudhof TC (1994) Synaptotagmin I: a major Ca2+ sensor for transmitter release at a central synapse. Cell 79:717–727
43. Li C, Ullrich B, Zhang JZ, Anderson RG, Brose N, Sudhof TC (1995) Ca(2+)-dependent and -independent activities of neural and non-neural synaptotagmins. Nature 375:594–599
44. Gerona RR, Larsen EC, Kowalchyk JA, Martin TF (2000) The C terminus of SNAP25 is essential for Ca(2+)-dependent binding of synaptotagmin to SNARE complexes. J Biol Chem 275:6328–6336
45. Davletov BA, Sudhof TC (1993) A single C2 domain from synaptotagmin I is sufficient for high affinity Ca2+/phospholipid binding. J Biol Chem 268:26386–26390
46. Chapman ER (2002) Synaptotagmin: a Ca(2+) sensor that triggers exocytosis? Nat Rev Mol Cell Biol 3:498–508
47. Berglund L, Hoffmann HJ, Dahl R, Petersen TE (1999) VAMP-1 has a highly variable C-terminus generated by alternative splicing. Biochem Biophys Res Commun 264:777–780
48. Isenmann S, Khew-Goodall Y, Gamble J, Vadas M, Wattenberg BW (1998) A splice-isoform of vesicle-associated membrane protein-1 (VAMP-1) contains a mitochondrial targeting signal. Mol Biol Cell 9:1649–1660
49. Sherry DM, Wang MM, Frishman LJ (2003) Differential distribution of vesicle associated membrane protein isoforms in the mouse retina. Mol Vis 9:673–688
50. Caicedo A, Herbert H (1993) Topography of descending projections from the inferior colliculus to auditory brainstem nuclei in the rat. J Comp Neurol 328:377–392